

Comparative Numerical Study of Turbulent Forced Convection in a Shell and Tube Heat Exchanger Between the Simple Case and With Cross Baffles

Ahmed Youcef, Rachid Saim

Laboratoire Energétique et Thermique Appliquée (ETAP), Département de Génie Mécanique, Faculté de Technologie, Université Abou Bekr Belkaid, Tlemcen Algeria
a_youcef83@yahoo.fr

Numerical investigations in two models of shell and tube heat exchangers are performed using CFD FLUENT commercial software based on the $k-\varepsilon$ model, the conservation equations of mass, momentum and energy are solved by the finite volume method. The dynamic and thermal behavior of the water circulating in the two-shell side will be analyzed in detail. The results show that the fluid is completely affected by the baffles, the velocity increases by 12% in the case without baffles and by 16% in the case with baffles, the heat transfer coefficient, the pressure drop, the total heat transfer rate, the pumping costs increase by 1,86% and 21,67% and 1,11%, and 21,68% successively.

1. Introduction

Forced convection in complex geometries finds its importance in various industrial fields and more particularly in nuclear reactors, heat exchangers, solar collectors, cooling of electronic components, shell and tube heat exchangers. Such work is of interest in improving the thermal performance of a shell and tube heat exchanger with baffle. In terms of study of the forms of chicanes, we quote the works of a comparative study between two types of heat exchangers with helical baffles and segmental baffles shows an increase in heat transfer coefficient and pressure drop about 44,1% and 56,1% successively to the second type (Li et al., 1989; Camaraza-Medina et al., 2018; Zhang et al., 2018), the heat transfer coefficient and the friction factor increase with the increase of the distance between the baffles (Zhang et al., 2009), after an experimental study showed the inclination angle 40° has better performances. (Du et al., 2014), the increasing to the number of the plates forming the baffle reduces the leakage flow and reduces the pressure drop. (Dong et al., 2014), have studied the heat transfer characteristics in a three-plate helical baffle heat exchanger, the results show that the local heat transfer coefficient on the central tube is much higher than the one of the peripheral tubes. (Nandan et al., 2016), performed a performance analysis of the injection of air bubbles at four different points in a tube-shell heat exchanger, the results show that the injection of air bubbles improves heat transfer by 25 to 40%. A comparative study of the performance of two different heat transfer enhancement configurations has been carried in this paper. The numerical simulation is proposed to study forced convection heat transfer characteristics for a Reynolds number $Re = 8939$ for the case with baffles is $Re = 2906$ for the simple case.

2. Problem definition

2.1 Geometry of the problem

The field of study, shown schematically in figure. 1, is a tubular heat exchanger equipped with seven tubes in the first case, and with two baffles having two overlapping sections in the second case, inside which flow the water with a mass flow of 1 Kg/s.

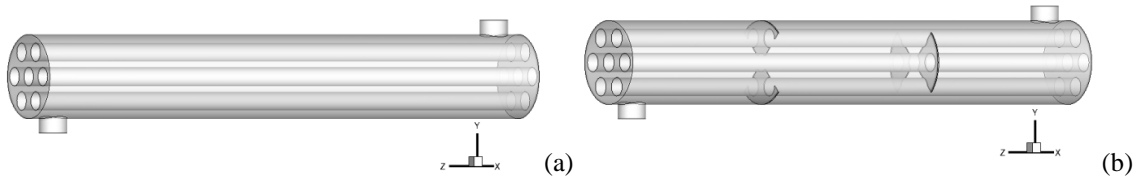


Figure 1: Geometry of the system under investigation (a) without baffles, (b) with baffles

Table 1: Geometric parameters

Parameter	Values
Shell size, D_s	90 mm
Tube outer diameter, d_o	20 mm
Tube bundle geometry and pitch	triangular, 30 mm
Number of tubes, N_t	7
Heat exchanger length, L	600 mm
Shell side inlet temperature, T	300°K
Baffle cut, B_c	36%
Number of baffles, N_b	2, $\alpha = 90^\circ$

2.2 Governing equations

To simulate the incompressible steady fluid flow and heat transfer, the governing flow equations, continuity, momentum and energy equations are written:

Continuity:

$$\frac{\partial(\rho u_i)}{\partial x_i} = 0 \quad (1)$$

Momentum:

$$\rho u_j \frac{\partial u_i}{\partial x_j} = -\frac{\partial P}{\partial x_i} + \frac{\partial}{\partial x_j} \left(\mu \frac{\partial u_i}{\partial x_j} - \overline{\rho u_i u_j} \right) \quad (2)$$

Energy:

$$\frac{\partial(\rho u_i T)}{\partial x_j} = \frac{\partial}{\partial x_j} \left(\left(\frac{\mu}{Pr} - \frac{\mu_t}{Pr_t} \right) \frac{\partial T}{\partial x_j} \right) \quad (3)$$

Turbulence kinetic energy k :

$$\rho u_j \frac{\partial k}{\partial x_j} = \frac{\partial}{\partial x_j} \left[\left(\mu + \frac{\mu_t}{\sigma_k} \right) \frac{\partial k}{\partial x_j} \right] + G_k - \rho \varepsilon \quad (4)$$

Energy dissipation ε :

$$\rho u_j \frac{\partial \varepsilon}{\partial x_j} = \frac{\partial}{\partial x_j} \left[\left(\mu + \frac{\mu_t}{\sigma_\varepsilon} \right) \frac{\partial \varepsilon}{\partial x_j} \right] + C_{1\varepsilon} \frac{\varepsilon}{k} G_k - C_{2\varepsilon} \rho \frac{\varepsilon^2}{k} \quad (5)$$

Turbulent viscosity:

$$\mu_t = \rho C_\mu \frac{k^2}{\varepsilon} \quad (6)$$

The turbulence production

$$G_k = -\overline{\rho u_i u_i} \frac{\partial u_j}{\partial x_i} \quad (7)$$

The model constants have the following values:

$C_{1\varepsilon}=1.44$, $C_{2\varepsilon}=1.92$, $C_\mu=0.09$, $\sigma_k=1.0$, $\sigma_\varepsilon=1.3$, et $Pr_t=0.09$.

3. Validation

3.1 Numerical model

The governing equations are iteratively solved by the finite volume method with the SIMPLE algorithm; the second-order upwind scheme is adopted for the momentum, energy, turbulence and its dissipation rate, default under-relaxation factors of the solver are used to control the update of the calculated variables for each iteration.

3.2 Grid sensitivity

The computational domain is meshed with unstructured hexahedral grid in the shell. A presentation of parameters in the section $y = 0.06\text{m}$ for a Reynolds number $Re=8939$ is illustrated in the following table.

Table 2: Dependence of the properties on the meshing size

Grid	U_{\max}	V_{\max}	W_{\max}	T_{\max}
227989	0,00005	1,6404	0,002	324,2547
573271	0,00006	1,6573	0,0023	324,4587
1075874	0,00007	1,6552	0,0022	324,3259

The results presented above show that the variation is very small and does not exceed 1%. The analysis of the results presented show that the choice of (1075874) elements, give a good prediction for the present numerical model.

3.3 Model validation

The results of the numerical simulation are employed to validate the models with the mass flow rate 0,5kg/s, 1kg/s, 2kg/s. A comparison of the numerical results and analytical data of the heat transfer coefficient (according to the Kern method) is presented in figure 2, the error between the numerical and analytical calculations average of 1,09%.

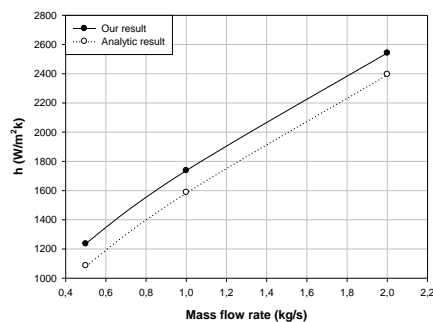


Figure 2: Average heat transfer coefficient

4. Resultants

The impact of baffles has two sections on the structure of the water flow in the shell and tube heat exchanger is presented for both dynamic and thermal aspects.

4.1 Hydrodynamic behavior

The velocity contour in the median longitudinal section ($x = 0\text{ m}$) for the two exchangers presented in Figure 3. For figure 3 (a), it is seen that the velocity is relatively uniform.

In figure 3 (b) it can be seen that the velocity of the fluid in the shell becomes relatively complicated and varies irregularly. In more detail when the fluid passes from a baffle, it is first accelerated quickly and then circulated

through the gaps with great velocity. This flow pattern is caused by periodic varied in the flow area that is induced by the disposition of the baffles.

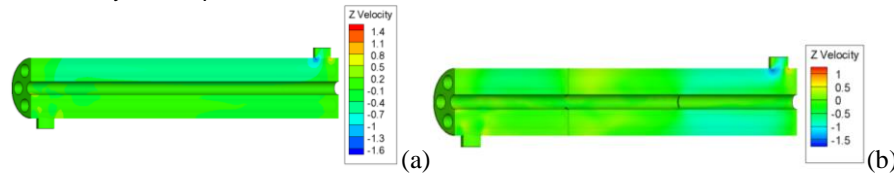


Figure 3: Velocity contours $x=0$ (a) without baffles (b) with baffles

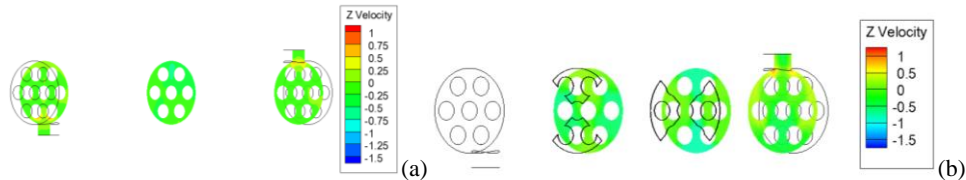


Figure 4: Velocity contours, (a) without baffles (b) with baffles

In figure 4 shows the transverse velocity contour in both exchangers. In figure 4 (a) the high transverse velocity found in the upper part of the shell. It can be seen in figure 4 (b) that the velocity is perfectly irregular along the shell and the fluid strongly affected by the baffle shape, therefore, an increase in velocity after the two baffles in the vicinity of the tubes. The higher velocity located between the two baffle sections and the tubes. A presentation of the velocity distribution along the two exchangers has the section $y = 0.04m$ illustrated in figure.

In figure 5 (a) shows a decrease in the velocity along the shell, the fluid does not encounter any obstacle, its velocity decreases due to the sudden enlargement and the lack of baffles. For figure 5 (b) the maximum velocity in the shell this product to the gaps of the baffles and the proximity of the tube, and at the outlet of the shell. The baffles produce recirculation zones of fluid resulting in a decrease in the flow velocity. The velocity of the flow in the shell for the case without baffle reaches maximum values of order of 12% of the initial velocity, and in the case with baffles reaches 16% of the initial velocity.

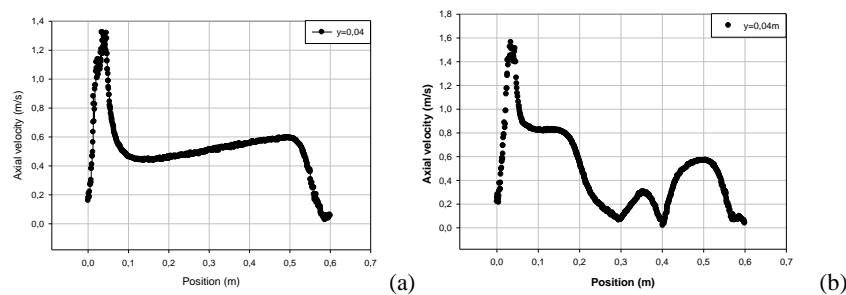


Figure 5: Velocity distribution at $y = 0.04m$; (a) without baffles, (b) with baffles.

4.2 Thermal behavior

In figure 6 (a) the fluid velocity is relatively low; therefore, the shell-side fluid is heated slowly and the outlet temperature is low. In figure 6 (b), the temperature varies after the baffles because the recirculation zones generated by the two section baffles. The figure 7 shows the temperature of the fluid in the cross sections in the two cases studied. it is observed that the temperature of the fluid changes much more rapidly along the direction of flow, and the outlet temperature is higher under the same inlet conditions, which confirms that the rate of convection transfer enhanced by the baffles.

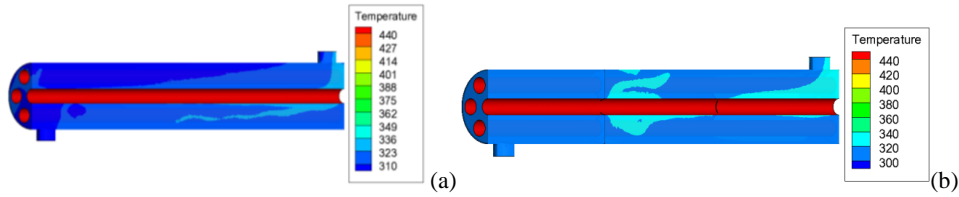


Figure 6: Temperature contours at $x = 0$, (a) without baffles, (b) with baffles

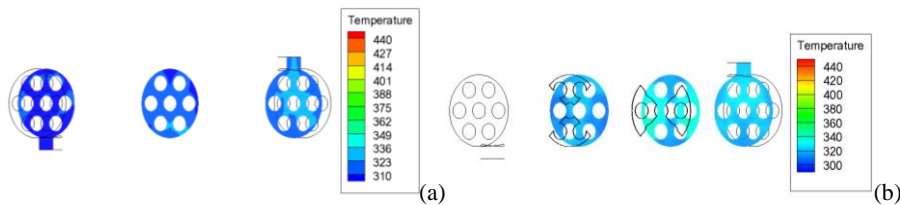


Figure 7: Temperature contours $z = 0.58m$; $z = 0.3m$; $z = 0.02m$, (a) without baffles, (b) with baffles

From figure 7 it can be seen that the two-section baffles, after the flow guidance in two paths, improve the turbulence intensity and the fluid temperature.

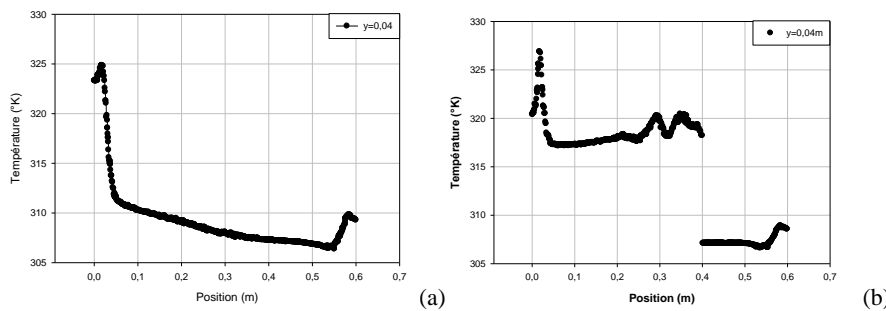


Figure 8: Temperature distribution at $y = 0.04m$, (a) without baffles, (b) with baffles

In Figure 8 (a) it is found that the fluid temperature increases slightly in the shell, the lack of baffles, is an additional factor of attenuation of the turbulence in the shell.

For figure 8 (b) it is found that in the regions after the baffle and the shell of the calender the temperature is increased sharply. The fluid temperature increases as soon as the fluid is again in contact with the baffle, because of the change in the direction of flow produced by the baffle, the highest value of the temperature appears behind the baffle. It is clearly observed that the temperature of the fluid changes much more rapidly after the first baffle ($z = 0.4 m$) in the direction of the flow as the temperature goes from $307.1 \text{ }^\circ\text{K}$ to $318.5 \text{ }^\circ\text{K}$, which confirms that the rate of convection transfer enhanced by baffles.

4.3 Performance of the heat exchangers

The table shows the evolution of the temperature, the heat transfer coefficient, the pressure drop, the total heat transfer rate, the pumping costs calculated in the two heat exchangers studied.

The heat transfer coefficient, the pressure drops, the total heat transfer rate, the pumping costs increase by 1,86% and 21,67% and 1,11%, and 21,68% successively.

Table 3: Performance of the heat exchangers

Parameter	Without baffles	With baffles
T ($^\circ\text{K}$)	322,51	324,2
h ($\text{W}/\text{m}^2\text{K}$)	954,66	1737
ΔP (pa)	18,79	395 ,3
Q (W)	94182	101228,6
P (kW)	0,019	0,4001

The baffle favors vortices over the simple flow case, and increasing the Reynolds number greatly increases the rate of heat transfer by introducing large recirculation zones.

5. Conclusion

A numerical study of the dynamic and thermal behavior of turbulent forced convection water flow in two heat exchangers was presented. The governing equations are solved using the finite volume method and the turbulence model $k-\epsilon$. The evolution of the axial velocity, the distribution of the temperature in selected sections are presented and analyzed.

The two secondary paths generated by the baffle are less vigorous compared to the single zigzag path created by the simple transverse baffle.

The high velocity generated by the baffle gaps in the shell intensively wash the walls of the three tubes at the first baffle and five tubes at the second baffle and result in a noticeable thermal improvement in the heat exchanger.

It is clear that the installation of two-section baffles varies the distribution of the temperature in the heat exchanger into three exchange zones, small, medium and large. Long operating life of the heat exchanger as the vibration induced by the flow is low in this case.

The optimum design of the heat exchangers largely depends on the configuration of the baffles. Two-section baffles represent an alternative to segmental baffles by circumventing their disadvantages. It is clear that the baffle installation of two sections varies the temperature in a remarkable way. The velocity increases because the overlapping configuration results in a reduction in the cross-flow area which causes an increase in velocity as the fluid passes through the high-velocity gap then launched out of the gap. The higher velocity located between the baffles and the tubes in the shell.

References

- Camaraza-Medina Y., Rubio-Gonzales Á.M., Cruz-Fonticiella O.M., García-Morales O.F., 2018, Simplified analysis of heat transfer through a finned tube bundle in air cooled condenser, *Mathematical Modelling of Engineering Problems*, 5(3), 237-242, DOI: 10.18280/mmep.050316
- Dong C., 2014, Influence of baffle configurations on flow and heat transfer characteristics of trisection helical baffle heat exchangers, *Energy Convers, Manage*, 88, 251–258.
- Du, W.J., 2014, Effects of shape and quantity of helical baffle on the shell-side heat transfer and flow performance of heat exchangers, *Chin, J, Chem, Eng*, 22, 243–251. DOI:10.1016/S1004-9541(14)60041-0
- Li H., Kottket, 1998, Effect of baffle spacing on pressure drop and local heat transfer in shell-and-tube heat exchangers for staggered tube arrangement, *International Journal of Heat and Mass Transfer*, 41, 10, 1303–1311. DOI: 10.1016/s0017-9310(97)00201-9
- Nandan A., Singh G., 2016, Experimental study of heat transfer rate in a shell and tube heat exchanger with air bubble injection (technical note), *International Journal of Engineering transactions B: Applications*, 29, 8, 1160-1166. DOI: 10.1016/j.enconman.2014.08.005
- Yang J.F., Lin Y.S., Ke H.B., Zeng M., Wang W.Q., 2016, Investigation on combined multiple shell-pass shell-and-tube heat exchanger with continuous helical baffles, *Energy*, 1-8. DOI: 10.1016/j.energy.2016.05.090
- Zhang J. F., 2009, Experimental performance comparison of shell-side heat transfer for shell-and-tube heat exchangers with middle-overlapped helical baffles and segmental baffles, *Chem, Eng., Sci*, 64, 1643–1653. DOI: 10.1016/j.ces.2008.12.018
- Zhang C., Guo Q., Sun J., Liu C., 2018, Comparative analysis for heat transfer performance of heat exchanger single tube model with and without plug-in, *Chemical Engineering Transactions*, 66, 301-306, DOI: 10.3303/CET1866051